Title
A Novel Approach to the Monitoring of the Human Gastrointestinal Tract

Author
Zegarski, Vincent William

Publication Date
2014

Peer reviewed|Thesis/dissertation

UNIVERSITY OF CALIFORNIA

Los Angeles

A Novel Approach to the Monitoring of the Human Gastrointestinal Tract

A thesis submitted in partial satisfaction

of the requirements for the degree Master of Science

in Electrical Engineering

by

Vincent William Zegarski

2014

ABSTRACT OF THE THESIS

A Novel Approach to the Monitoring

of the Human Gastrointestinal Tract

by

Vincent William Zegarski

Master of Science in Electrical Engineering

University of California, Los Angeles, 2014

Professor William J. Kaiser, Chair

Suffered by one in four patients who undergo abdominal surgery, postoperative ileus is a condition where the gastrointestinal tract shuts down and bowel function is halted. With the onset of this condition, patients cannot tolerate any advancement in their diet, and should be restricted from any oral ingestion. However, patients are occasionally fed before it is determined that ileus is present, which can lead to a wide range of complications and further prolong the patient's hospital stay. With proper detection, a patient's dietary schedule can be modified to improve recovery, increasing overall patient comfort and safety. A novel system, *AbStats*, is presented that records the sounds emitted from the abdomen and autonomously detects those that are indicative of digestive activity. Initial investigations from clinical trials show that the rate of

peristalsis events is a clear indicator of digestive health and can be used to identify patients who are experiencing postoperative ileus. Furthermore, an algorithm has been developed to detect these events while simultaneously rejecting noise that can lead to the misinterpretation of a recording. Overall, by providing extended recordings and advanced detection methods, the *AbStats* system will change how physicians monitor the human gastrointestinal tract today.

The thesis of Vincent William Zegarski is approved.

Robert N. Candler

Gregory J. Pottie

William J. Kaiser, Committee Chair

University of California, Los Angeles

2014

Table of Contents

Acknowledgements

With so many people responsible for my success in the Masters program and in this exciting project, I must start by sincerely thanking my advisor, Dr. William Kaiser Ph.D. His guidance, enthusiasm, and encouragement have been paramount in the success I have experienced in these last two years.

Next, thank you to Dr. Brennan Spiegel M.D., Dr. Mark Pimentel M.D., and their amazing teams for being the trail-blazers for this technology, spreading the word of its capabilities to the medical field, contributing critical insight on the human digestive system, and coordinating the invaluable trials at the hospitals local to UCLA.

I am very lucky to be part of the great Wireless Health Institute, which is filled with wonderfully intelligent and purely amazing people. A special thank you must go to Digvijay Singh for his amazingly fast and quality work in the gateway development, as well as all of his help with other tasks including prototype development, system design, coordination for clinical trials, and so much more.

Finally, and most importantly, a heart-filled thank you to my family for your continued support and love. Knowing you are always there for me has allowed me to push myself and be the person who I am proud to be today and I am eternally grateful for all of the opportunities you have given me.

Chapter 1. Introduction

Following abdominal surgery, patients typically suffer from the inhibition of bowel function in a condition known as postoperative ileus (POI). Upwards of one in four patients who undergo surgeries in the abdominal region—such as a colectomy, the resection of any portion of the large intestine (colon)—experience some form of POI [1]. While not considered to be life threatening, POI can cause a family of potential complications, including an increase in the patient's length of stay (LOS) in the hospital and overall patient discomfort [2]. In addition to increased abdominal pain, complications that patients may experience include nausea and vomiting, possibly leading to aspiration pneumonia caused by breathing liquid or food into the lungs. Nationwide, abdominal surgeries result in 1.8 million hospital days and cost a total of $1.75 billion annually, where patients with POI have a 30% longer LOS than those without. Reducing the average LOS can save in medical costs as well as help to clear up hospital resources, which is especially critical in hospitals where there is a high-demand for emergency procedures.

The human gastrointestinal (GI) tract is shown below in Figure 1. Bowel function is ultimately categorized as the movement of chyme, the semi-solid masses that are expelled by the stomach into the duodenum [3]. The presence of bowel sounds indicates bowel function, as do the proceeding bowel movements or passing of flatus. Bowel motility is typically performed by peristalsis, the powerful contraction and relaxation of the smooth bowel muscles to push contents down the gastrointestinal tract. These peristalsis events are the main source of the sounds indicative of digestion and thus can aid in the verification of proper bowel function, and conversely, the absence of these events can help in the detection of ileus.

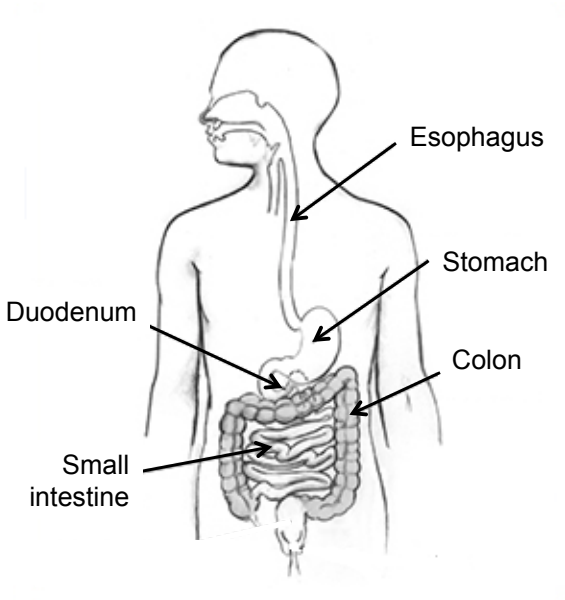

Figure 1: The Human Gastrointestinal Tract [4]

After abdominal surgery, hospitals can elect to prohibit the patient to ingest any solids or liquids, *nil per os* (NPO), for the first and second postoperative days (POD), followed by a period consisting of a liquid-only diet, and then the progression to solid food. More commonly, aggressive "fast-tract" recovery schemes allow liquids on POD zero once the patient is awake from anesthesia. However, a recovery plan that is too aggressive when a patient suffers from POI can lead to many of the complications described earlier, which is met by returning the patient to the NPO restriction. On the other hand, if POI is not present, the patient may not be able to receive proper nutrition and can experience further discomfort when NPO is extended and diet is slowly advanced. The progression in healing cannot be observed without conducting an examination that uses a stethoscope to hear the peristalsis events indicative of proper bowel function. A fixed timetable for a patient's diet is typically followed until severe problems arise.

Due to the high patient to caretaker ratio, POI monitoring is limited to short and infrequent visits by attending physicians and nurses who are unable to devote a significant

amount of time listening to a patient's abdomen. Depending on the level of bowel functionality, peristalsis events may not occur frequently enough to be heard in these short examinations, which can lead to an inaccurate estimate of digestive health. Ultimately, there is clear need for prolonged monitoring of the GI tract that can only be met by an automated system capable of detecting the presence of, as well as analyze, digestive sounds.

A novel system for abdominal monitoring, aptly named *AbStats*, has been developed as a means to provide extended monitoring of postoperative patients and aid in dietary progression at appropriate times by proper detection of POI. By properly identifying the sounds that result from peristalsis events—those that are indicative of bowl function—an event rate can be calculated to accurately identify POI and monitor GI health.

An automated system that can listen to the abdomen, such as *AbStats*, can easily be deployed from extended periods of time to monitor and track the progression of a patient's health, two traits that are unmet in the current paradigm of digestive medicine. While extensive research such as [5], [6], and [7] can be found on recordings of peristalsis events and the migrating motor complex (MMC)—a system-wide series of periodic and less-powerful events to help "clean out" the GI tract—no system has previously been developed to autonomously indicate when and how frequently these occur.

This thesis will outline the latest complete *AbStats* system, including the hardware used to record of the abdominal sounds and the algorithms used to analyze the acquired data. With initial designs including multiple custom circuits, the incorporation of high-quality "off-the-shelf" parts has allowed the majority of the gateway—the central hub of the system—to be assembled without soldering, as all connections are made by secure connectors. As a result, future manufacturing can be streamlined, and performance will be held constant at a high level.

Also, a specialized sensor has been designed to collect the sounds emitted by the patient's digestive system. In addition to matching the performance of $200 digital stethoscopes, this sensor was created to be inexpensive and disposable, as to remove the risk of contamination between patients that increase the risk of infections and an even longer hospital LOS. Finally, an algorithm was created to distinguish the sounds that are indicative of digestive activity, capable of identify signals of interest while removing potentially harmful noise from the recording.

AbStats underwent thorough testing internally with healthy subjects (HS) after which it was then deployed in nearby hospitals for IRB-reviewed clinical trials. By manually analyzing recordings, the algorithm was tuned to accurately identify events of interest while properly handling injected noise. As a result, sounds heard when a patient is experiencing some level of digestion are identified and marked in recordings autonomously, providing the basis for a revolutionary method that will change the way doctors monitor and treat postoperative ileus worldwide.

Chapter 2. Data Acquisition System Design

2.1 Overview

The data acquisition system is composed of two main components: the gateway and the disposable sensors. The gateway holds all of the hardware needed to collect the audio recordings and was designed as a reusable device capable of recording numerous patients throughout its lifetime as a bedside unit. Depending on what configuration the physician desires to use, there will be between one and four disposable sensors connected to the gateway and affixed to the patient's abdomen. A diagram showing the gateway and two disposable sensors is illustrated below in Figure 2. An Ethernet cable is available for a personal computer (PC) to connect to the gateway through Secure Shell (SSH). However, the gateway only needs to be plugged-in to a common wall outlet during operation and does not always need to be connected to a PC—it is able to act as its own stand-alone device that continuously records the sounds emitted from the patient's abdomen.

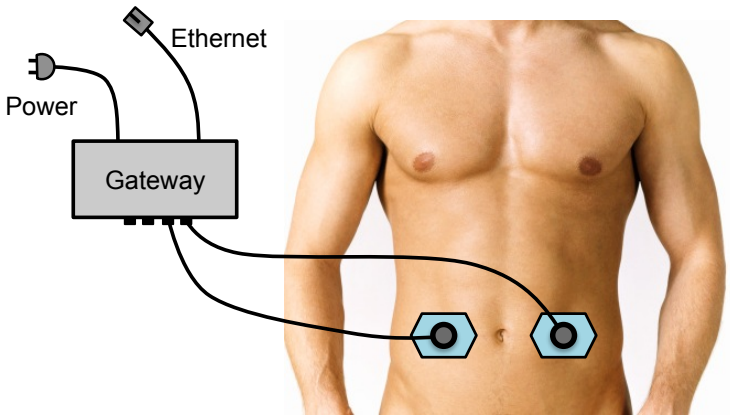

Figure 2: Diagram of Data Acquisition System with Two Sensors Affixed to Patient

The sensors are intended for one-time use only and are discarded to prevent the risk of contamination from patient to patient. A common configuration includes two sensors being placed a few centimeters from the navel on the lower abdomen to record the sounds that originate from the peristalsis events in the small intestine. Physicians can decide to move the sensors to other locations and change the number of sensors used to better target specific regions in the GI Tract. The following sections will provide more information by going into further detail about the design of gateway and the disposable sensors that make up the data acquisition system.

2.2 The Gateway

The *AbStats* Gateway is the central hub for data acquisition and is responsible for recording the sounds emitted from the patient's abdomen. In addition to sampling the sensors that are connected to the audio ports and creating the .wav files, the gateway will analyze the audio recordings and save pertinent information that can be used by the physician to detect ileus and monitor GI health. The gateway, as seen in Figure 3, has a hard plastic housing that keeps all of the internal hardware secure from being damaged when the system is moved from patient to patient throughout a hospital. The case measures 9 inches (22.9cm) by 5 inches (12.7cm), and is 2 inches (5.1cm) thick.

Figure 3: The Gateway

The architecture of the gateway hardware, including the internal connections as well as the input and output ports, is shown below in Figure 4. Special effort was made to find modules that were "off-the-shelf" and to have the connections be as tidy as possible. This simplicity will allow many gateways to be manufactured with ease, where cost will be reduced by limiting the number of custom hardware and minimizing the labor necessary for assembly.

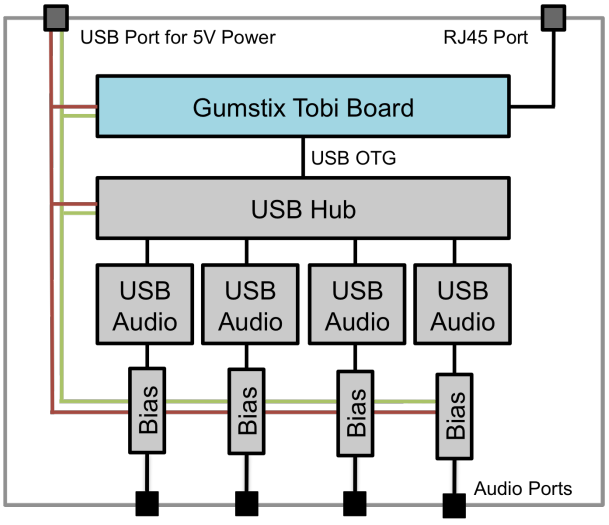

Figure 4: Gateway Architecture

A single USB cable powers every module within the gateway with a medical-grade AC adapter that can be plugged in to a common wall outlet. This provides a consistent 5V DC supply—low power compared to many of the diagnostic tools typically found in a hospital—for the Gumstix Tobi board, USB hub, and the biasing circuits. The entire gateway uses 5W of power on average, which can spike up to 10W during the boot-up process. With this low power consumption, a battery can be incorporated into the design to provide hours of monitoring, allowing patients to continue the recording even when they are out of bed. All of the modules inside the gateway have their own internal regulators that reduce the 5V supply to a voltage necessary to function, as well as help provide a more robust supply for each that is free from noise that can reduce audio signal quality.

The ARM-based Gumstix Tobi board enables the processes needed for the recording, storage, and analysis of uncompressed .wav audio files. The data acquisition system runs on 2-minute cycles in which 110-second .wav files are recorded and all other processes—storing, analyzing, and the recording of results—must be completed in the final 10 seconds before the next recording cycle can begin. If these other processes surpass the 10-second limit, the subsequent cycle will be delayed until necessary resources are available to begin recording. A configuration file determines which combination of the four audio ports the gateway will record from. It provides the capability for other recording features, such as recording length and sample rate, to be modified. This configuration file, as well as other log files and audio recordings, can be viewed by using SSH from a computer connected through the RJ-45 port.

When a physician reviews a recording at the end of the day, it is essential for them to know precisely when each file was generated. Rather than listen to all the recorded audio files, this review can be performed quickly by visually inspecting plots of the recorded waveforms, as

seen later throughout this thesis, or by noting the rate of detected digestive events. The acquisition time will allow patient information to be linked to the recordings by documenting when each test was administered in the patient's medical chart. A real-time clock (RTC) on the Gumstix board is used to keep an accurate account of the audio recording times; for each .wav file, the time when the recording begins is noted in a designated timestamp file. The RTC is capable of keeping the current time for up to a month, even when power isn't supplied to the system, by using a coin-cell battery so the current date and time need not be set every time the system is started [8]. When the gateway is plugged into a wall outlet, the current time is noted and recording begins on the channels specified in the configuration file.

A disposable sensor is plugged into the appropriate audio port when a channel is recording. This sensor must be biased using the biasing circuit, which is connected to the USB audio interface to sample the signal. All of the USB audio interfaces are connected to the USB hub and through USB *On-The-Go*, the USB hub is connected to the Gumstix Tobi board. The USB audio interface provides superior audio quality to the two built-in 3-conductor (stereo) 3.5mm audio jacks on the Gumstix board and its USB-based setup allows for more than two sensors to be simultaneously recorded, adding flexibility to the system's capabilities. An earlier design attempted to have a pair of sensors share the ground line, allowing the sensors to each supply one of the channels to make a "stereo" recording. However, this proved to increase the complexity of disposable sensor design as well as introduce limits in sensor capabilities.

As previously mentioned, a biasing circuit must be included for the audio recordings. While these are commonly included within the sensor themselves, to reduce the cost of each disposable sensor, the biasing circuit was included past each 3.5mm audio jacks inside the gateway, as shown in the gateway architecture above in Figure 4.

The schematic for each of the bias circuits is seen below in Figure 5. The three signals that go to and from the disposable sensor are the biased audio signal, ground, and the vibrating motor control line, which is explained further in Section 2.3.

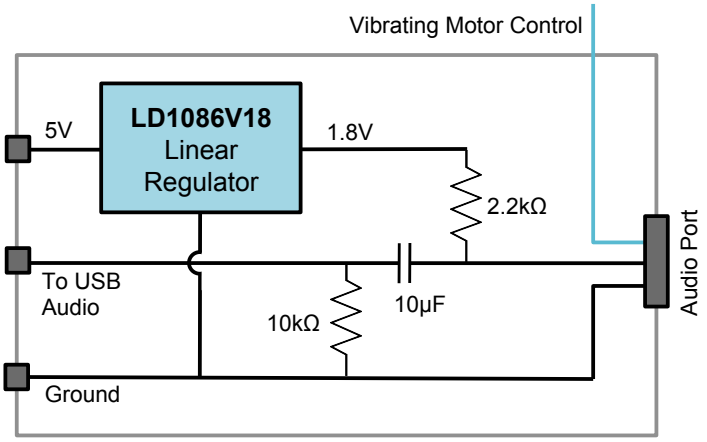

Figure 5: Biasing Circuit for One of Four Audio Channels

The biasing circuit takes the 5V DC that is used throughout the Gateway and reduces it down to 1.8V using a LD1086V18 linear regulator [9]. This circuit supplies the necessary power to turn-on the internal field effect transistor (FET) as well as providing a load that is adequate for the SPL XCM6035 microphone [10]. A linear regulator is ideal for this noise-sensitive application because it provides a consistent voltage without introducing artifacts commonly seen in switching regulators, such as voltage spikes or periodic noise at the switching frequency [11]. The reduction in electrical noise comes at a higher power cost, but is an acceptable trade-off since this system is connected directly to a wall outlet and power was not a constraining factor in system design. Any noise that is injected into the biasing of the electret microphone will certainly be seen in the recorded files and add difficulty to the already nontrivial task of separating digestive events from environmental noise.

2.3 Disposable Sensors

Inspiration for the disposable sensor design came from the same stethoscopes that are used by physicians in hospitals today, like that shown below in Figure 6.

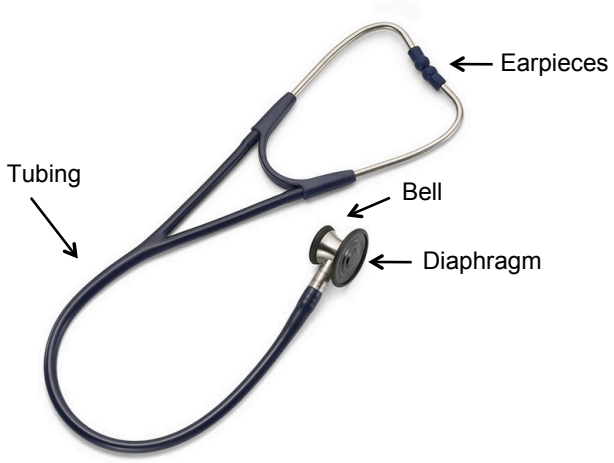

Figure 6: Welch Allyn Harvey Stethoscope [12]

The head of the stethoscope has a wide diaphragm compared to the small earpieces, causing the collected sounds to be amplified and easier for the user to hear. By studying this amplification, a design that consisted of a diaphragm and microphone inside of a plastic housing, similar to how the tubing is connected to the stethoscope bell, was proposed to collect the sounds that are emitted from a patient's abdomen.

When a digestive event occurs in the stomach, whether it is a peristalsis event by the intestines or the movement of gas in the stomach, sound waves will propagate away from the origin and will transfer through the abdomen and out of the body. When this propagation occurs and reaches the surface, the patient's skin will vibrate due to the sound (pressure) waves. With the sensor housing attached to the patient's abdomen such that it creates a sealed enclosure, the skin will act as the sensor's diaphragm, which then moves as sound passes through. This

diaphragm, the abdomen surface, will enclose the plastic housing and movements change the pressure inside the housing, which will then be *heard* by a microphone. This process is similar to the change in pressure inside the stethoscope tubing as the result of changing pressure in the bell.

A side-view and a top-view of the sensor design are shown in Figure 7 below. At the base of the plastic housing—made from a plastic end-cap typically used for furniture—are two washers with an inner-diameter (ID) equal to that of the housing. These washers are glued to *Tegaderm* transparent-film dressing (bandages) to allow proper adhering to the patient's abdomen that is strong enough to hold the disposable sensor in place, while still being breathable and comfortable to wear for an extended period of time.

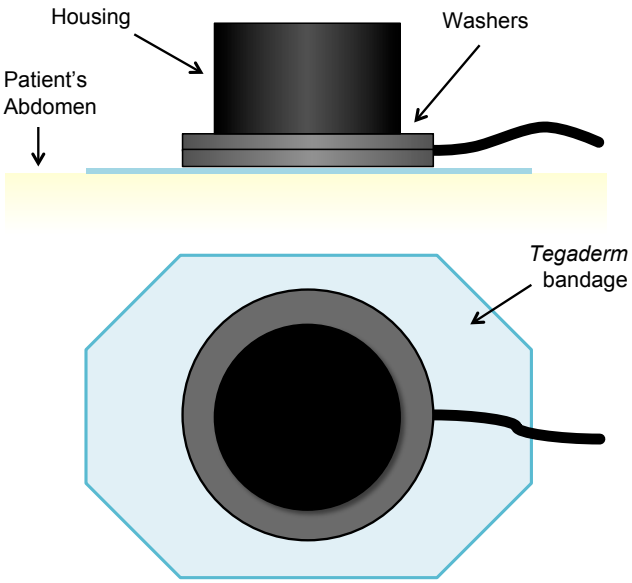

Figure 7: Diagram of a Disposable Sensor. Side View (top) and Ariel View (bottom)

Tegaderm bandages are used to affix the sensor to the patient's abdomen. It is important that the sensor is tightly coupled to the patient's abdomen to create an airtight seal. Small coin-cell vibrating motors are added to every sensor to equip them for coupling tests, a method that is

further described in Section 2.3.2. A photo of a disposable sensor, along with a US quarter for size reference, after it is assembled and ready for use is shown below in Figure 8.

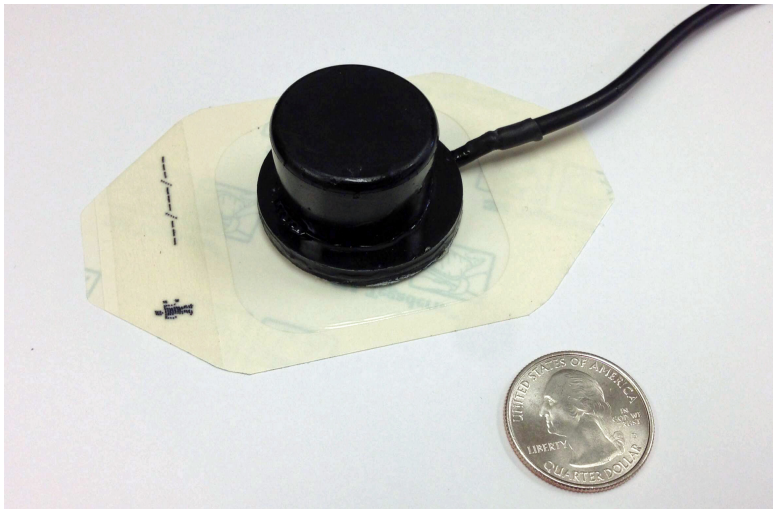

Figure 8: Photo of a Single Disposable Sensor

Inside the sensor housing, a circular prototyping board is used to hold the electric microphone and vibrating motor. This board keeps these internal components neat—physicians and business sponsors may see inside the housing and expect a professional appearance—as well as simplifies assembly of these disposable sensors, improving labor costs and keeping quality consistent.

2.3.1 Electret Microphone

The electret microphone used in the disposable sensor must be capable of capturing most of the audible frequency range, which ranges from 20Hz to 20kHz in humans. This requirement was set for two main reasons. First, since *AbStats* is intended to "listen" to a patient's abdomen, with the goal of identifying the sounds indicative of digestive function as a physician would, the human audible range is a desirable fit. Also, the sounds emitted during peristalsis are in the low frequencies, approximately between 80Hz and 200Hz, which is covered by microphones intended for human speech and hearing. With the frequency range in mind, an electret was

chosen that provided a stable frequency response and, equally importantly, was very inexpensive. Since the sensors must be disposable, cost is a driving factor in design and must be considered when selecting a model to incorporate.

The 6mm diameter, 3.5mm tall electret microphone that was chosen to be inside the plastic housing of the disposable sensor is the XCM6035 from SPL, pictured below in Figure 9. Wires can be soldered on to the two pads on the back of the microphone, where the light green side is the negative (ground) terminal. The signal collected by the electret microphone is then sent to the biasing circuit in the gateway before it is sampled by the USB audio module.

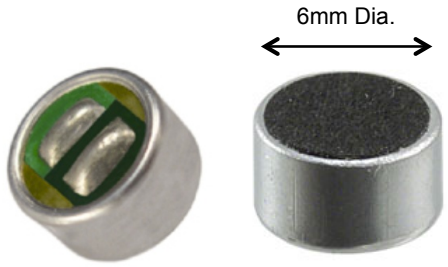

Figure 9: Photo of the XCM6035 Electret Microphone. Back (left) and Face (right)

This electret microphone provides a stable frequency response that covers most of the audible range, as seen in Figure 10 [10]. In the signal processing stage, which is described in Chapter 3, the recorded data is filter using a high-pass filter (HPF) with a cutoff frequency of 40Hz and low-pass filter (LPF) with a cutoff frequency of 300Hz to focus on the frequency range of interest and remove any electrical noise that may have been introduced into the signal. With this under consideration, a microphone where the frequency response covers 40Hz and greater is sufficient.

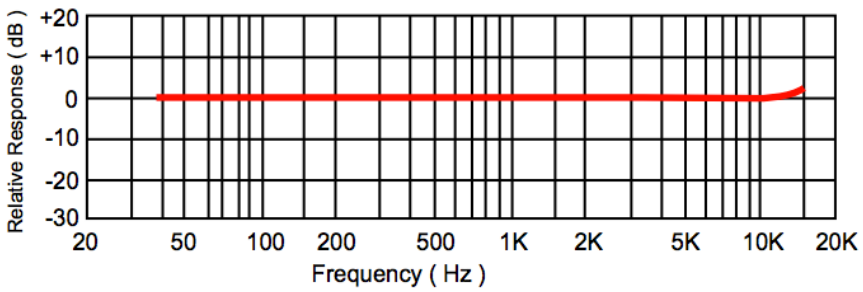

Figure 10: Frequency Response of XCM6035 Electret Condenser Microphone

The datasheet [10] also provides a schematic for the microphone, which has been presented below in Figure 11. In addition to what is inside the microphone package, this diagram shows the load resistor (RL) and bypass capacitor (C) that should be placed between the two terminals of the package and the inputs of the audio recorder. This is the same configuration as that presented when the biasing circuits were explained previously in section 2.2.

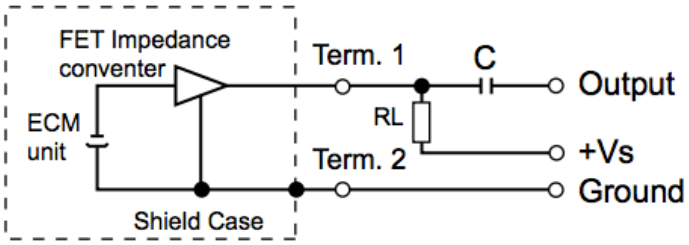

Figure 11: Schematic of the XCM6035 Electret Condenser Microphone with External Bias Circuit Added

With the electret microphone fully explained, now it is time to investigate the other electronics component in the disposable sensor—the vibrating motor.

2.3.2 Vibrating Motor

The vibrating motor is a critical component in the disposable sensor, as it warns against improper coupling between the sensor and the patient's abdomen. The motor chosen for this is pictured below in Figure 12. This 10mm diameter motor is made by Parallax, and requires less than 3V

DC voltage to be applied across the leads to produce a vibration. As the voltage applied increases up to 3V, the rate at which the motor spins increases up to 9,000 RPM. To provide the voltage to the motor, one terminal is connected to ground of the electret microphone, while the other is connected to an analog-out pin of the Gumstix Tobi board. The audio signal, vibrating motor driving line, and ground are connected to the gateway via a 3-conductor 3.5mm audio jack.

Figure 12: Photo of Parallax Vibrating Motor

During a sensor-coupling test, there must be at least two sensors affixed to the patient's abdomen. Let's consider the situation where there are two sensors, like shown earlier in Figure 2. The left sensor is the receiver and will be recording during the test. The right sensor is the transmitter and will emit a short 20ms vibration.

By analyzing the brief audio file that was recorded by the left sensor, we can determine whether or not *both* sensor are properly coupled. Poor signal quality in this file suggests that one or both of the sensors are loose and must be adjusted. For completeness, each sensor in a configuration will in turn be the transmitter, and only after every set has passed will the system declare that all sensors are properly coupled.

It is very important to verify that the sensors that are recording the patient's abdomen are not loose, especially while attempting to detect or monitor POI. Loose sensors will likely not detect all, or possibly any, of the signals emitted from the GI Tract. A situation where the sensor is loose and the patient's POI has concluded may result with a delay in his/her diet progression, a longer LOS, and further discomfort as a result of a false-positive diagnosis.

2.3.3 Ensuring Sanitary Conditions

Since the sensor will commonly be placed on the abdomen of patients who have recently undergone abdominal surgery, it may be in contact with non-intact skin such as an incision. Such items in the hospital are considered *semi-critical items* and must undergo high-level disinfection or sterilization before they can be reused [13]. Due to the construction of the sensor housing, including the small crevices where bacteria can build-up, it is extremely difficult to guarantee that the sensor has been properly cleaned. Because it is not practical to require this level of cleaning on each sensor between patient use, and with the cost of materials and assembly reduced significantly, disposability is notably a superior feature. In addition to limiting the sensors' lifetime to a single use, materials such as adhesives are required to be of high quality (medical grade) due to their direct contact with patients.

Chapter 3. Motility Event Detection

3.1 Overview

Analysis of each .wav file must be completed accurately and efficiently. As mentioned previously in Chapter 2, there is only ten seconds for the embedded processor to save, analyze, and record pertinent information regarding the 110-second signal. The goal during the analysis portion is to properly identify the bowel sounds in the abdomen that indicate that digestion is occurring.

While there are many different candidates of sounds that can be indicative of digestive health, peristalsis events cause very distinctive *pops* to be emitted that are unlike any other sounds recorded during initial investigations, including: taps to the disposable sensor, electronic noise, voice, or patient movement. By counting these intense contractions of the small intestine, a metric can be devised that indicates the activity, and ultimately health, of a patient. However, proper steps must be taken to ensure that any of these other sounds are not counted as peristalsis events, which would introduce an error in the results of the audio signal analysis.

3.2 Definition of the Peristalsis Event Signal in Recordings

The unique popping sounds that originate during peristalsis events are distinguishable when they are plotted with respect to time. These events can be thought of as pseudo-impulse signals, as the pops have very large amplitude for a very short duration. A typical “impulse-like” peristalsis

event can be seen below in Figure 13, where a 200ms recording excerpt of a healthy subject's abdomen has been captured.

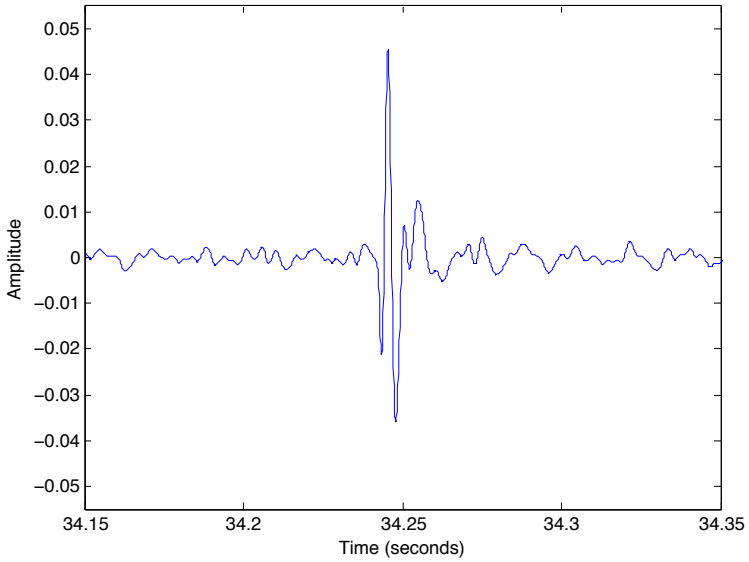

Figure 13: A Typical Peristalsis Event

This peristalsis event is composed of only two spikes—or possibly three, depending on where the distinction is made—before it quickly dampens back to the noise floor. Spikes, or peaks, will be defined by the portions of the signal that are above a certain amplitude threshold (Ath) for any amount of time. To see the uniqueness of this signal, compare it to some of the noises that are likely to be found in abdomen recordings such as cloth rubbing against the sensor head or speech by person nearby or the patient. Longer 400ms excerpts of recordings showing such noise sources can be seen in Figure 14 and Figure 15. Amongst other distinguishing factors, the duration of these noise events is significantly longer than the impulse-like peristalsis event and can be a quick indicator that these sounds differ.

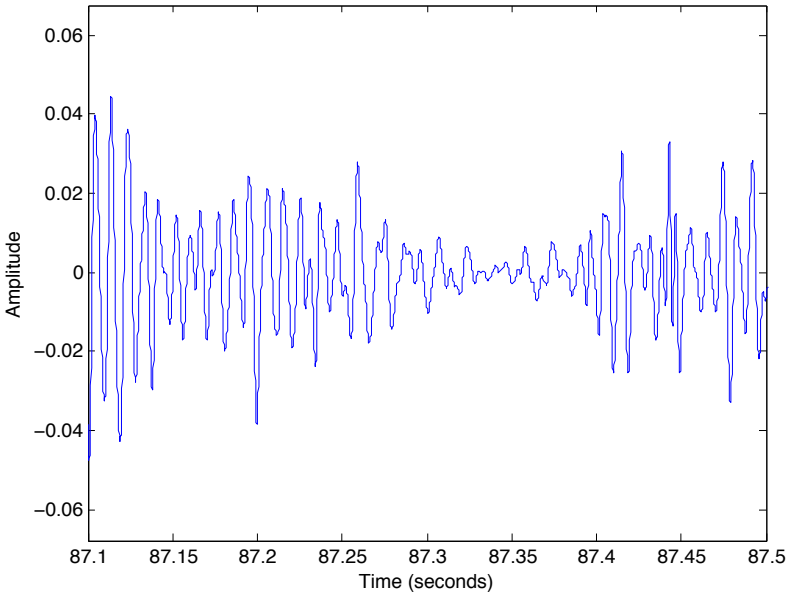

Figure 14: Noise from Cloth Rubbing Against Sensor Head

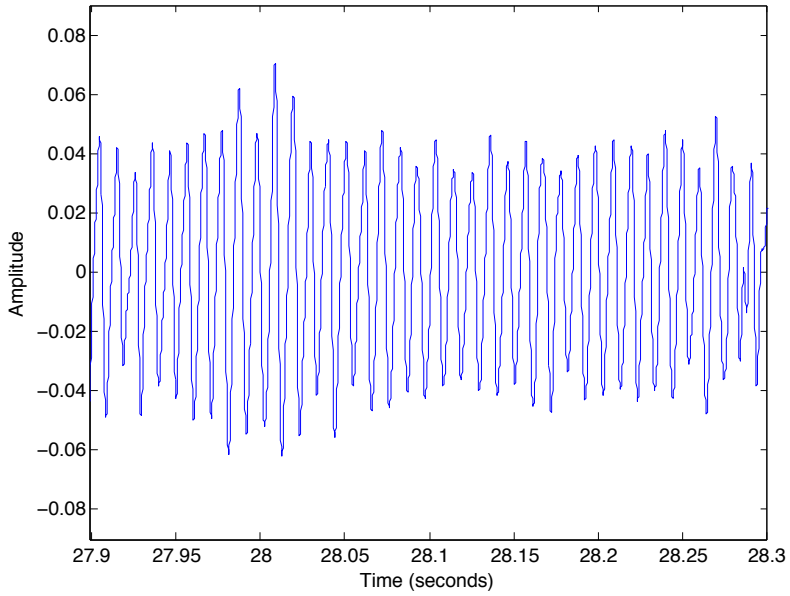

Figure 15: Noise from Nearby Speech

From these differences, a set of *rules* can be developed that a small portion of an audio wave must follow in order to be marked and counted as a peristalsis event.

Using the typical peristalsis event seen in Figure 13, an empirically devised set of heuristics can guide the development of the detection algorithm. Peristalsis events seem to follow a certain set of rules:

1. There should be no less than 2 and no more than 3 “big” peaks (portions of signal that are above a set amplitude threshold and greater than one-third of the maximum peak amplitude) grouped together.
2. Each peak width must be within a certain range (not too narrow and not too wide in time).
3. Adjacent peaks need to be close to each other, without a large time gap in-between.
4. Before the first peak and after the last peak, the signal should remain below Ath for a relatively long duration.

Figure 13 is redrawn below in Figure 16 with each rule illustrated at least once to better show which portion of the signal it is checking. By using figures like this, the parameters that define the rules above can be set and tuned to obtain an accurate event detector.

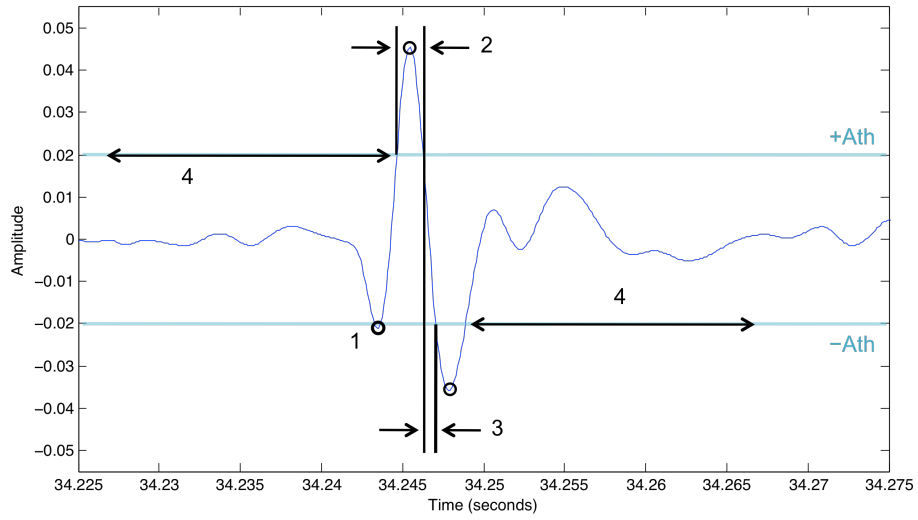

Figure 16: Peristalsis Event with Rules Illustrated

With these rules established, and the parameters that define them in place, the peristalsis (impulse-like) event detection algorithm can be developed and implemented in a tool such as MATLAB. It is important to note that these rules are not an exhaustive list of steps needed for signal analysis, but is simply a definition for the type of signal that the system is looking for and counting in the recordings of the patient's abdomen.

3.3 Algorithm Implementation

The algorithm to detect the impulse-like peristalsis events must be able to accurately identify the portions of the signal that follow all the rules defining such an event, excluding noise such as speech or sensor movement.

The strict set of rules described above will prove to be very useful in gaiting out much of the noise that can be found in a recording taken in non-ideal conditions, such as a noisy hospital room where the patient is being spoken to by physicians, nurses, and guests. However, more steps must be made to ensure the signal is clean enough to accurately detect the impulse-like events.

3.3.1 Preprocessing

After the .wav file is loaded, where each sample is spaced from the next by the sampling period 1/fs, it is down sampled by a factor of 1/Q to change the effective sampling rate to fs/Q. This is done when the recordings were taken at a high sampling rate, far above the necessary limit for processing low frequency signals. Next, a set of filters is applied to remove low- and high-frequency electronic noise that may have been superimposed to the recording. Both are

implemented as 4th-order Butterworth filters, where the cutoff frequencies for the high-pass filter and low-pass filter are 40Hz and 300Hz respectively, which is the frequency band of interest for the sounds emitted during peristalsis events. The resulting frequency response is shown below in Figure 17.

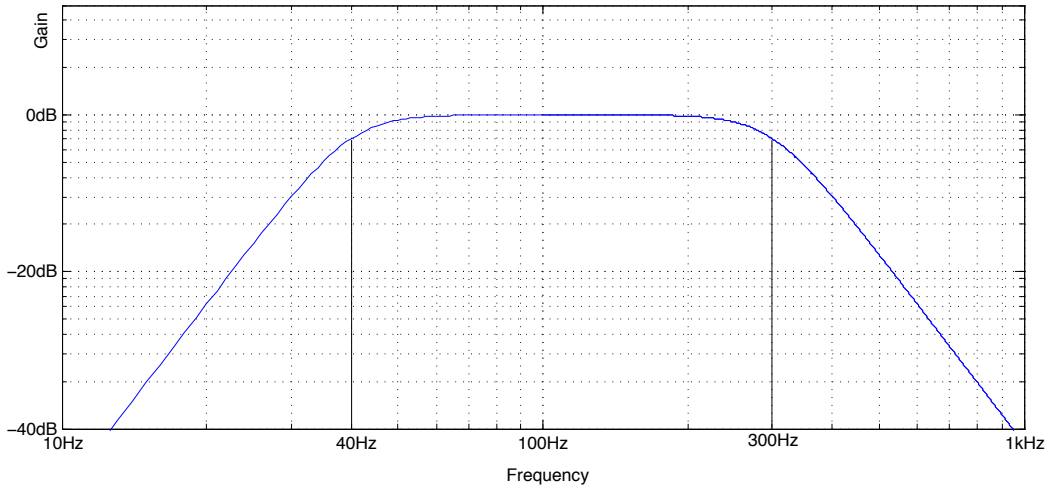

Figure 17: Frequency Response of Filters

Next, any bias that may have been introduced in the system is removed by removing the mean of the samples of the entire recording. Typically, this offset is small and is at least an order of magnitude less than the noise floor of the signal, but is always removed as a preventative measure. Furthermore, if this offset is comparable to the noise floor or maximum amplitude of the recording, then there is likely a problem in the system that must be addressed urgently.

3.3.2 Checking File for Periods of Noise

With the electronic noise removed by the cascaded high-pass and low-pass filters, the algorithm now turns its focus to checking for sections in the recording that resemble noise. As mentioned previously, although there will be a strict set of rules in detecting the sounds of interest

(peristalsis events), it is beneficial to remove segments that are overwhelmed by noise—speech, movement, sensor touching, etc.

The signal is partitioned into 50ms windows, which have 50% overlap with neighboring windows. For each window, starting at index *i* with a with of *n* samples, the power is calculated as:

$$P_{window} = \frac{1}{n} \sum_{i}^{i+n-1} y^2(i)$$

By calculating the power for each window, the algorithm looks for many consecutive windows that have high power. Because we are looking for short, impulse-like events, these consecutive high-power windows are likely to be noise, and these periods should be ignored when searching for sounds corresponding to peristalsis events.

Figure 18 below is an example of this power-based noise removal algorithm at work. The top plot shows four taps (72-76 seconds) followed by a period of rubbing cloth against the sensor head (76-84 seconds) and finally a short period of speech (86-87 seconds). The power is plotted against a log-scale in the middle plot, which is high in amplitude during the described noisy regions. Once a set number of consecutive windows are above a threshold, the whole region is marked as noise (red line) and all samples are set to zero, resulting in the "cleaned" signal on the bottom plot. It should be noted that this recording was taken to test and demonstrate the noise detection algorithm. In a quiet room where the patient is still and not talking, there may not be a single window that passes above the power threshold and no part of the signal will need to be cleaned.

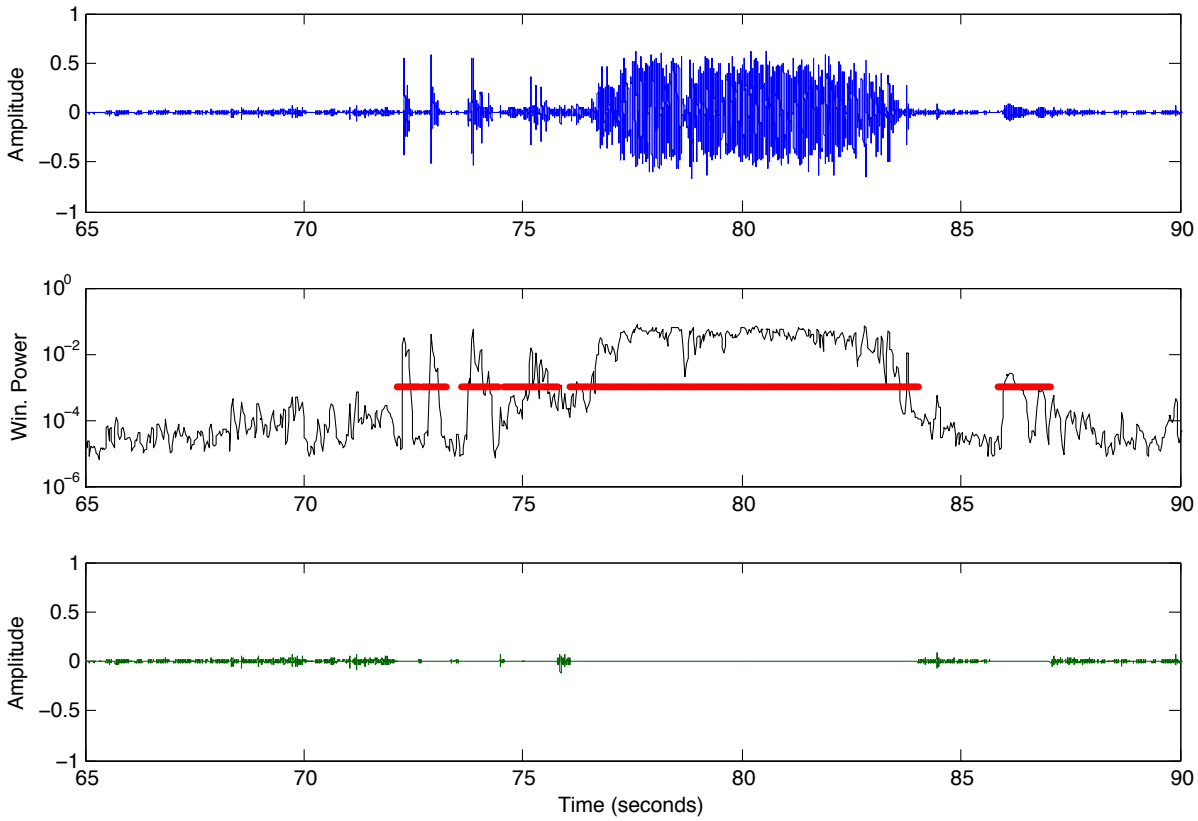

Figure 18: Example of Noise Being Removed from Abdomen Recording

Conversely, a quiet 5-second excerpt of a recording that has three of the desired impulse events at 70.9, 71.8, and 73.7 seconds is seen below in Figure 19. While the power increases when the windows pass over the impulse events, it quickly returns down to the nominal amount and there are no instances where many consecutive windows have high power. Note that there are no red markings to indicate noise being detected.

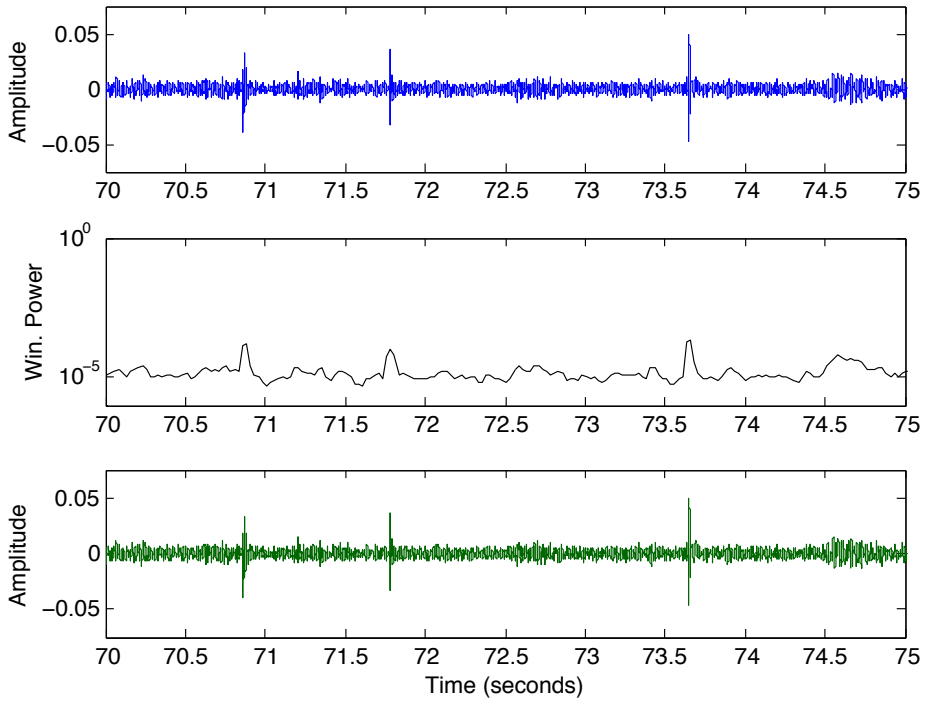

Figure 19: Window Power in Clean Recording with Three Impulse-Like Events

Now, with the majority of the noise removed, the recording is ready to be searched for the sounds indicative of peristalsis events—the impulse-like signals described earlier.

3.3.3 Detecting the Signals of Interest

Recall from the definition of the peristalsis events, and the rules that can be used to define them, that the model event can be described by the peaks and their proximity to others. From this, it is clear that the first step is to find all points in the audio recording where peaks occur—when the amplitude of a group of samples is above the threshold.

For each peak, the algorithm must find the times where the peak begins—the signal amplitude transitions from below to above Ath—and where the peak ends—the signal amplitude

transitions back down below Ath. This method is similar to detecting a zero-crossing (ZC) in speech processing. A "rising" threshold crossing, which defines a peak beginning, can be defined when $y(i) \geq \text{Ath}$ & $y(i\text{-}1) < \text{Ath}$, where $y(i)$ is the i-th sample of the signal y. Similarly, the "falling" threshold crossing, which defines a peak ending, is where $y(i) < \text{Ath}$ & $y(i\text{-}1) \geq \text{Ath}$. Each peak beginning and ending can be marked by the time at which they occur, $t(i)$, which is then calculated as i/fs, where fs is the sampling frequency of the audio recorder, 44.1kSamples/s before being down sampled in software.

With the time information of every peak in the audio recording collected, groups of peaks can now be formed as potential peristalsis events, with each being checked against all of the rules defined earlier. Groups are formed by collecting the peaks that are within certain proximity of each other, usually where the time between peaks is less than 0.1 seconds. This grouping insures that there are "quiet periods" on either side of an event, if it is found that the group follows the rules to be determined a peristalsis event.

Each group of peaks is checked against the peristalsis event detection criteria. First, the amplitude of each peak is normalized to the largest peak, and peaks that are greater than 1/3 are considered as "big" peaks. The number of big peaks is what is checked in Rule 1 and if this is not within the predetermined range, the group is rejected and deemed to not be a peristalsis event.

If the group has the correct number of big peaks, the proximity of the peaks will be checked to ensure they are close enough to each other without large periods of time separating them. This is done using the beginning and ending times found during peak discovery. As before, if a group does not pass this rule-check, it is rejected as possibly being a peristalsis originated impulse-like event.

The remaining groups of peaks that were not rejected all follow the rules that define impulse-like events that are typical of peristalsis. These groups are counted and a rate such as events-per-minute or events-per-second is calculated to be stored in the data file that will be used by the physician for determining the health of the patient. If any noise is found earlier by the window-power noise-detection method, that specific portion of the signal is removed and the total signal time when the event rate is calculated is reduced to provide an accurate report, even though the recording quality was compromised.

3.3.4 Summary of Signal Processing and Analysis

All of the steps necessary to process the abdominal recordings—loading, preprocessing, event detection, and result recording—can be summarized by the flow chart below in Figure 20.

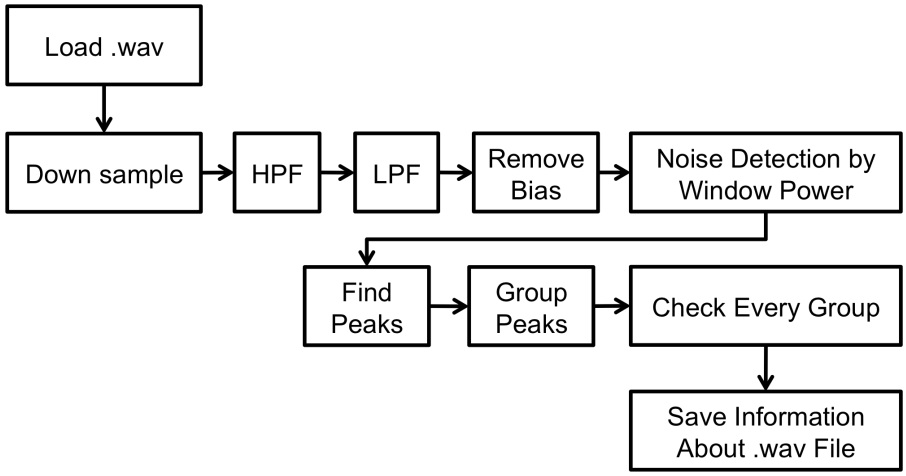

Figure 20: Process for the Analysis of Abdominal Recordings

MATLAB provides many benefits when developing this event-detection algorithm, including quick implementation and powerful figure generation. However, this algorithm must be able to execute on an embedded system, specifically the Gumstix Tobi board that is in the *AbStats*

gateway. Therefore, this algorithm must be converted to C and compiled for the ARM-based platform.

3.4 Conversion of Algorithm to C for Embedded Use

The conversion from MATLAB to another high-level programming language can introduce many bugs if it is not properly planned and executed. A majority of the impulse event detection algorithm was developed with this transition from MATLAB to C in mind and as a result, the algorithm was manually converted successfully in a short period of time.

As mentioned earlier, a benefit of the MATLAB implementation of the algorithm is its versatility and power in visualizing the data collected. This ease-of-use allows parameters—minimum and maximum number of peaks in a group, peak separation requirements, acceptable range of peak width, etc.—to be modified for optimal results. These parameters can then be modified in the C implementation to obtain the same detection abilities. To ensure that both algorithms are performing identically, extensive log files (see Appendix A) are saved and can be compared to each other to discover differences that may be present. A difference in the log files would be an indicator that a bug is present in one, or both, of the algorithm implementations. Obtaining identical results requires that both implementations perform each step in the algorithm flow by the same method, and thus produce the same count of impulse-like peristalsis events.

Inconsistencies between the two implementations might occur during the filtering of data. In MATLAB, the use of the `y=filter(B,A,x)` function allows a signal x to be filtered to create y, as defined by the polynomials B and A. This filter is implemented internally by a tapped delay line (TDL) filter, which is used for both the high-pass filter and the low-pass filter

[14]. For a 4th-order filter, like that used in the two filters described in Section 3.3.1, each filtered sample $y(n)$ is found by:

$$A(0)y(n) = B(0)x(n) + B(1)x(n-1) + B(2)x(n-2) + B(3)x(n-3) + B(4)x(n-4)$$
$$-A(1)y(n-1) - A(2)y(n-2) - A(3)y(n-3) - A(4)y(n-4)$$

The coefficients in A are normalized so that $A(0) = 1$ to further simplify the calculation of $y(n)$. With the insight to what this filtering function is doing internally, an alternate function `myfilter` can be created in both MATLAB and C that single handedly replaces both filters, as MATLAB's filter function is not available to be used in C.

Another internal MATLAB function that is not initially available in C is the means to load a .wav file, `wavread`. However, the `sndfile` library provides the methods necessary to load a .wav file into an array, which can then be searched for peaks to be grouped, as outlined in the algorithm above [15].

With the modifications necessary for the conversion from MATLAB to C in place, there are now two versions ideal for parameter modification and in-field implementation. The C code only needs to be cross-compiled so that it can be executed in the ARM-based Gumstix for real-time analysis of patient abdomen recordings.

Chapter 4. Results

4.1 Investigations on Sounds Originating from the Abdomen

Extensive investigations were conducted to determine whether the impulse events were a suitable indicator of digestive health. During initial testing, it was confirmed that the "pops" that originate from the intestine peristalsis events were frequently heard in all healthy subjects who have eaten relatively recently. However, while this showed that these events are heard across healthy patients, it didn't yet prove the contrary: that the complete absence of peristalsis events indicated POI.

Over 80 patients in the Gastrointestinal Diseases section of the Veterans Affairs (VA) West Los Angeles Healthcare Center were consented and fit with an early version of the *AbStats* system to collect a database of recordings on a wide range of conditions. Included in this sample were 19 inflicted with POI and 9 who have returned back to normal nutrition and/or were diagnosed as having a healthy digestive system. From this n = 28 subset, images were created to visualize the recorded 110-second audio files and allow the impulse-like events to be manually counted. Figure 21 below is one of the waveforms recorded in this trial, where the first 10 seconds is omitted, as this is when the vibrating motor was turned on for coupling verification.

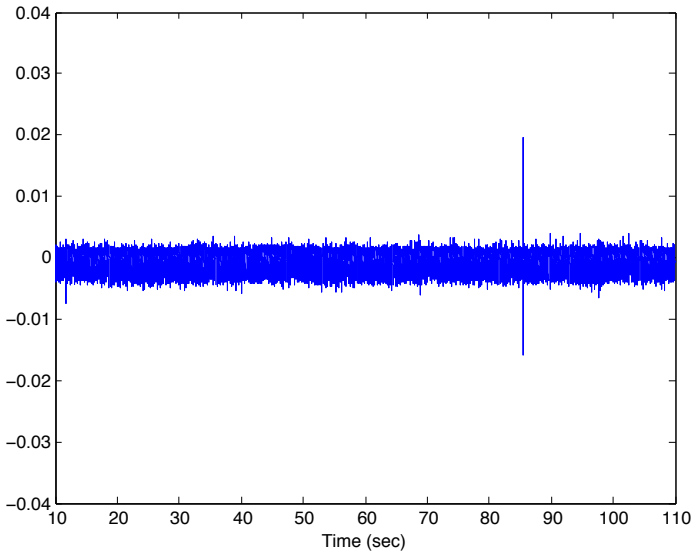

Figure 21: Recorded Waveform

An example of the desired impulse-like event is seen at approximately 84 seconds from the beginning of the recording. This example occurred in one of the healthy subjects and is a great template showing what these events looked like when the entire recordings were viewed. Events similar to this were counted to calculate event rates for each patient. Table 1 summarizes the resulting event rates for the 19 postoperative ileus patients as well as the 9 healthy subjects.

	Postoperative Ileus	Normal Nutrition or HS
Min	0.002	0.097
1st Q	0.004	0.130
Median	0.010	0.141
3rd Q	0.015	0.155
Max	0.022	0.178

Table 1: Summary of Manual Event Counting and Resulting Rate Calculation

To better illustrate this data, a box-and-whisker plot is presented in Figure 22 below.

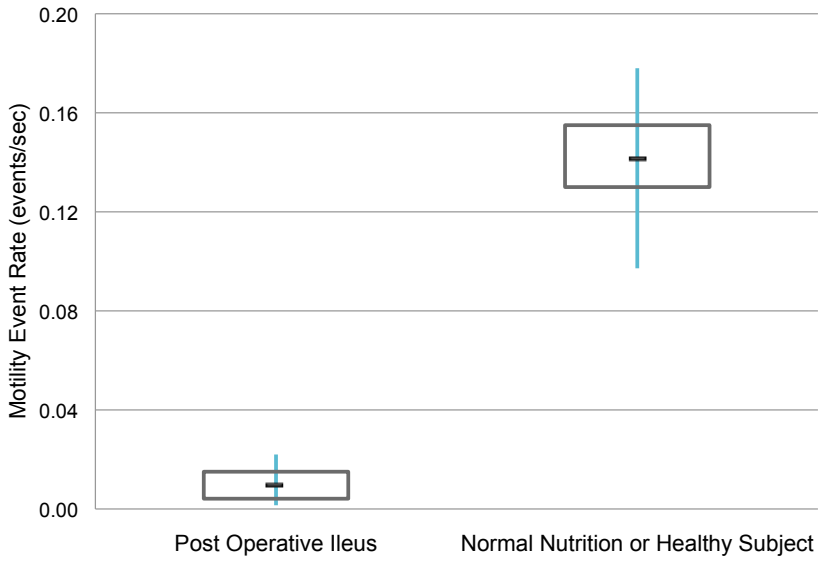

Figure 22: Box-and-Whisker Plot of Event Rate for POI Patients vs. HS

One promising result that can be rapidly seen on this plot is that there isn't any overlap between the digestive event rate for POI and HS groups. The impulse-like peristalsis events are in fact a promising indicator of digestive health, and a low event rate is certainly indicative of POI in patients.

4.2 Verifying Automated Detection of Peristalsis Events

With the evidence suggesting that the presence of impulse-like peristalsis sounds indicate activity in the digestive system, the algorithm that detects these signals must be verified. The implementation in MATLAB plotted excerpts of the signal so that each group of peaks in a .wav file could be visualized. This made it possible to confirm that each of those that were found to be peristalsis events were similar to that presented earlier in Figure 13.

Two examples of groups that were marked as being peristalsis events are shown below in Figure 23. The yellow lines indicate where the positive and negative amplitude threshold, Ath.

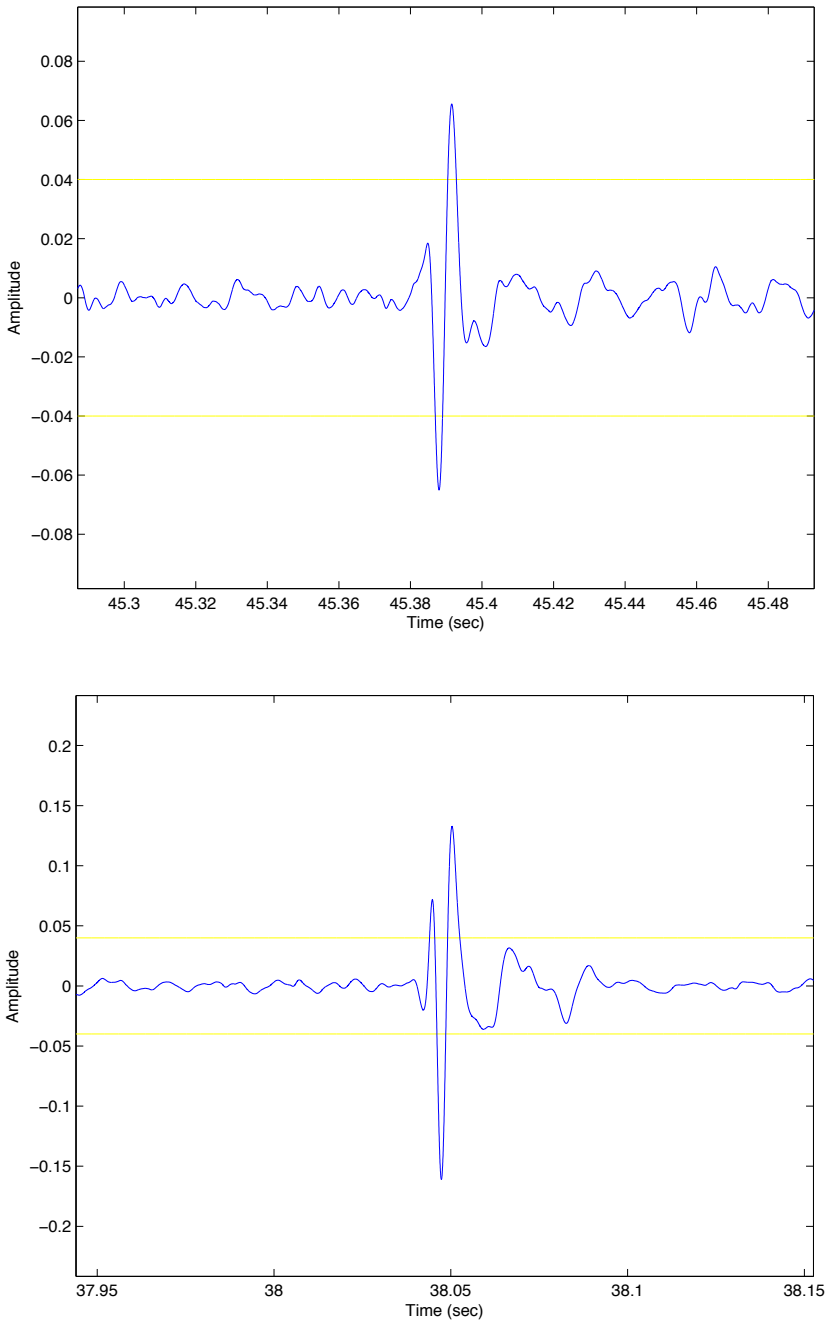

Figure 23: Two Examples of Detected Peristalsis Events

Both of these examples follow all four rules described in section 3.2. They both have the proper number of peaks, where each peak is the appropriate width and adequately close to the adjacent

peaks, and there are long periods before and after the group where no other peaks occur. An equally important step in the verification process is to ensure that the groups that are rejected—the groups of peaks that were not considered to be a peristalsis event—do not follow the rules or even appear to be similar to the template impulse-like signal described earlier.

Figure 24 below is an example of a group that was rejected by the peristalsis event detection algorithm.

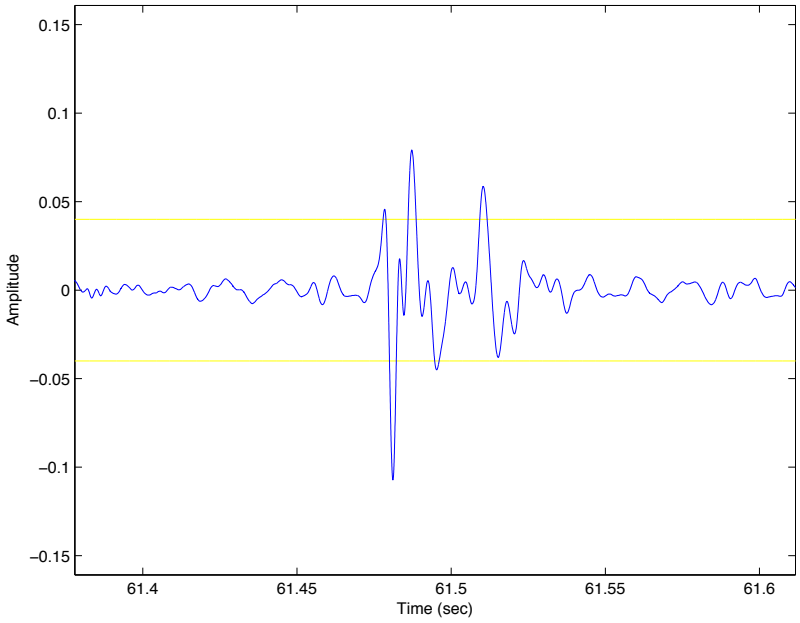

Figure 24: Rejected Group Found to not be a Peristalsis Event

Details about each group of peaks are included in the log files that are saved by the peristalsis event detection algorithm. The following is an excerpt from the log file, specifically for this rejected group:

```
Group 63: peak index 161 to 165, time 61.478 to 61.512 sec
0.42    1.00    0.74    0.42    0.55
---> rejected (wrong number of big peaks)
---> rejected (big peaks spaced too far)
---> rejected (big peaks spaced too far)
verdict: group is rejected, not a good event
```

This log file excerpt provides the following information: the time of the group in which this information correlates to, the normalized magnitudes of the peaks within the group, notes generated from the rule check, and the final decision to whether or not the group is an impulse-like peristalsis event.

Immediately, by viewing Figure 24, it is evident that this group does not follow the template described earlier. The group does not have the correct number of peaks and these peaks are not adequately close to each other. This is also indicated by the log file, which then suggests that the algorithm is properly rejecting groups that do not follow the rules to classify impulse-like peristalsis events described in section 3.2.

Another example of a group that was rejected is shown below in Figure 25. Similar to the previous instance, this group has too many peaks that are also too far from each other.

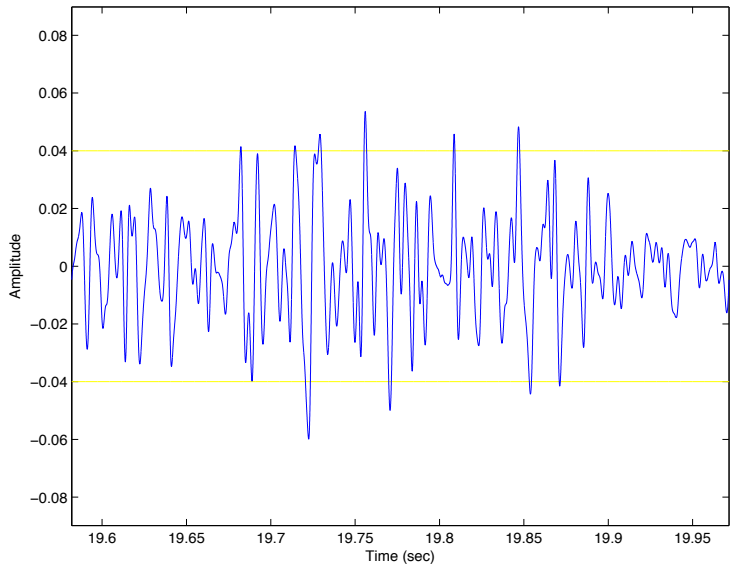

Figure 25: Rejected Group Found to not be a Peristalsis Event

This rejected group of peaks is perhaps a case where noise may have not been detected by the window-power stage described earlier, but still did not result in a false-positive detection.

Chapter 5. Conclusions and Future Work

This thesis presented a system capable of recording the sounds emitted from patient's abdomen by the use of non-invasive, disposable sensor for an extended period of time. Peristalsis events cause sharp impulse-like "pops" and are indicators of digestive system activity. An algorithm was developed to autonomously detect these events, and was verified using recordings taken from in-lab healthy subjects.

Currently, the latest version of the *AbStats* system is collecting more data at the VA West Los Angeles Healthcare Center and Ronald Reagan UCLA Medical Center. These recordings will allow the autonomous algorithm to be tuned to most accurately detect the impulse-like events critical to diagnosing POI. Simultaneously, final adjustments to the system are being made so that the first version of *AbStats* that will provide information to the physicians directly—rather than only recording abdominal sounds—will be ready for deployment in the near future.

While early work has focused on the detection of POI in patients, this is certainly not the limit of this system. Future work includes expanding the capability of the system by developing more classifiers to monitor and diagnose a wide range of gastrointestinal disorders such as irritable bowel syndrome (IBS). In addition to the development of novel algorithms, there will be new prototypes developed to meet the need for further monitoring when a patient is not in the hospital, specifically designed for in-home and everyday mobile use. Additional features, including a touch-sensitive screen, will be added to these devices to allow user input and provide continuous feedback on patient data and the condition of the recording system.

There is an ever-growing need for a system like *AbStats* in hospitals today, as physicians are eager to obtain as much pertinent data on their patients as possible. The work presented here showed the basis for this technology, spanning from introductory investigations on the acoustic emissions from the human abdomen, to the hardware and software developments.

Appendix A. Excerpt from a Sample Log File

Below is an excerpt from a log file created as a debugging tool for the impulse-event detection algorithm. Included in this log is a header of tunable parameters, window power outputs, and rule checking for each group of peaks. The end of the file indicates how many peristalsis events were found and at what time in the .wav file they occur.

```
file: /Volumes/whi2/AbStats/sample_files/clean_02.wav

Ath:                    0.040
start time:             0.0 sec
end time:               0.0 sec
downsample (P/Q):       1/5
effective fs:           8820.0 samples/sec
removed bias:           0.0000000789

window width:           0.0500 sec
window stagger:         0.50
high power threshold:   0.000500
consec. hi-P limit:     3
pre- and pos-cursors:   3, 3 windows

min group spacing:      0.100 sec
ratio to be big pk:     0.333
peaks in group:         2 min, 3 max
peak width:             0.0010 sec min, 0.0100 sec max
max peak separation:    0.0050 sec

zero-indexed.

------------------------------------------------------------


indx start -    end   | time start -   end        | power of window | flags
i:       0 -     441  | t:   0.000 -   0.050 sec  | p: 0.000000000  |
i:     221 -     662  | t:   0.025 -   0.075 sec  | p: 0.000000000  |
i:     442 -     883  | t:   0.050 -   0.100 sec  | p: 0.000000000  |
i:     663 -    1104  | t:   0.075 -   0.125 sec  | p: 0.000000000  |
i:     884 -    1325  | t:   0.100 -   0.150 sec  | p: 0.000000000  |
i:    1105 -    1546  | t:   0.125 -   0.175 sec  | p: 0.000000000  |
i:    1326 -    1767  | t:   0.150 -   0.200 sec  | p: 0.000000000  |
i:    1547 -    1988  | t:   0.175 -   0.225 sec  | p: 0.000000000  |
.
.
.
i:  968201 -  968642  | t: 109.773 - 109.823 sec  | p: 0.000056165  |
i:  968422 -  968863  | t: 109.798 - 109.848 sec  | p: 0.000015108  |
i:  968643 -  969084  | t: 109.823 - 109.873 sec  | p: 0.000010192  |
i:  968864 -  969305  | t: 109.849 - 109.899 sec  | p: 0.000013610  |
i:  969085 -  969526  | t: 109.874 - 109.924 sec  | p: 0.000011632  |
i:  969306 -  969747  | t: 109.899 - 109.949 sec  | p: 0.000004257  |
i:  969527 -  969968  | t: 109.924 - 109.974 sec  | p: 0.000003833  |
i:  969748 -  970189  | t: 109.949 - 109.999 sec  | p: 0.000006875  |
```

```
Finished finding window power.

223 peak beginnings and 223 peak endings found.

Grouped the peaks into 89 groups.


Group 0: peak index 0 to 1, time 0.379 to 0.384 sec
1.00    1.00
verdict: group is good event


Group 1: peak index 2 to 3, time 0.513 to 0.518 sec
1.00    0.84
verdict: group is good event


Group 2: peak index 4 to 8, time 1.106 to 1.124 sec
0.45    1.00    0.99    0.42    0.42
---> rejected (wrong number of big peaks)
verdict: group is rejected, not a good event


Group 3: peak index 9 to 10, time 1.342 to 1.347 sec
0.92    1.00
verdict: group is good event


Group 4: peak index 11 to 13, time 1.841 to 1.854 sec
0.73    1.00    0.50
verdict: group is good event


Group 5: peak index 14 to 15, time 2.020 to 2.027 sec
1.00    0.90
verdict: group is good event


Group 6: peak index 16 to 18, time 2.249 to 2.260 sec
1.00    0.89    0.40
verdict: group is good event


.
.
.


Group 78: peak index 203 to 203, time 81.401 to 81.401 sec
1.00
---> rejected (wrong number of big peaks)
verdict: group is rejected, not a good event


Group 79: peak index 204 to 205, time 82.504 to 82.509 sec
1.00    0.90
verdict: group is good event


Group 80: peak index 206 to 207, time 83.011 to 83.015 sec
0.75    1.00
verdict: group is good event
```

```
Group 81: peak index 208 to 209, time 84.867 to 84.871 sec
1.00    0.87
verdict: group is good event


Group 82: peak index 210 to 211, time 85.068 to 85.073 sec
0.99    1.00
verdict: group is good event


Group 83: peak index 212 to 212, time 86.324 to 86.324 sec
1.00
---> rejected (wrong number of big peaks)
verdict: group is rejected, not a good event


Group 84: peak index 213 to 213, time 86.723 to 86.723 sec
1.00
---> rejected (wrong number of big peaks)
verdict: group is rejected, not a good event


Group 85: peak index 214 to 217, time 95.805 to 95.830 sec
0.71    0.85    0.90    1.00
---> rejected (wrong number of big peaks)
---> rejected (big peaks spaced too far)
verdict: group is rejected, not a good event


Group 86: peak index 218 to 219, time 100.083 to 100.087 sec
1.00    0.83
verdict: group is good event


Group 87: peak index 220 to 221, time 107.832 to 107.837 sec
0.89    1.00
verdict: group is good event


Group 88: peak index 222 to 222, time 108.323 to 108.324 sec
1.00
---> rejected (wrong number of big peaks)
verdict: group is rejected, not a good event




Found 60 events.

0.382 sec.
0.516 sec.
1.345 sec.
1.848 sec.
2.023 sec.
2.255 sec.
3.670 sec.
3.965 sec.
4.222 sec.
4.427 sec.
4.579 sec.
4.763 sec.
5.738 sec.
6.024 sec.
7.416 sec.
8.348 sec.
8.550 sec.
12.622 sec.
16.780 sec.
```

```
17.826 sec.
18.401 sec.
21.865 sec.
22.060 sec.
22.207 sec.
22.564 sec.
27.880 sec.
28.819 sec.
28.995 sec.
30.428 sec.
30.954 sec.
33.662 sec.
33.844 sec.
34.022 sec.
34.208 sec.
36.584 sec.
37.905 sec.
38.075 sec.
38.270 sec.
41.392 sec.
46.664 sec.
50.100 sec.
57.159 sec.
57.320 sec.
57.567 sec.
58.227 sec.
60.496 sec.
60.621 sec.
61.080 sec.
61.296 sec.
65.815 sec.
69.286 sec.
69.743 sec.
73.650 sec.
80.146 sec.
82.507 sec.
83.013 sec.
84.869 sec.
85.070 sec.
100.085 sec.
107.834 sec.


Done.
```

References

[1] T. Asgeirsson, et al. *Postoperative Ileus: It Costs More Than You Expect*. Journal of the American College of Surgeons, Vol. 210, No. 2 (February 2010), pp. 228-231.

[2] A. J. Senagore. *Pathogenesis and clinical and economic consequences of postoperative ileus.* American Journal of Health-System Pharmacy, Vol. 64 (October 2007), pp. 53-57.

[3] E. H. Livingston and E. P. Passaro Jr. *Postoperative Ileus*. Digestive Diseases and Sciences, Vol. 35, No. 1 (January 1990), pp. 121-132.

[4] *Bleeding in the Digestive Tract*. National Digestive Diseases Information Clearinghouse, National Institute of Diabetes and Digestive and Kidney Diseases, National Institutes of Health, Bethesda, MD (2013).
Available: http://digestive.niddk.nih.gov/ddiseases/pubs/bleeding/.

[5] H. J. Ehrlein and M. Schemann. *Gastrointestinal Motility*. Technical University of Munich, Munich, Germany.

[6] R. Ranta, et al. *A Complete Toolbox for Abdominal Sounds Signal Processing and Analysis*. 3rd European Medical and Biological Engineering Conference IFMBE-EMBEC (2005).

[7] J. D. Hardcastle and C. V. Mann. *Study of large bowel peristalsis*. Gut (1968).

[8] *Tobi*. Gumstix, Portola Valley, CA (2014).
Available: https://store.gumstix.com/index.php/products/230/

[9] *LD1086: An adjustable and fixed low drop positive voltage regulator*, Rev. 32. STMicroelectronics, Geneva, Switzerland (2013).

[10] *Electret Condenser Microphone: XCM6035 series* Datasheet. SPL, Hong Kong (2008).

[11] *Linear & Switching Voltage Regulator Handbook.* Rev. 4. ON Semiconductor, Phoenix, AZ (February 2002).

[12] *Welch Allyn Harvey DLX Double Head Stethoscope Navy*. Steels, Saint Joseph, MI (2014). Available: http://www.steeles.com/products/welch-allyn-harvey-double-head-stethoscope-5079-327.

[13] *Cleaning, Disinfection, and Sterilization.* California Department of Public Health, California (2013). Available: http://www.cdph.ca.gov/programs/hai/Documents/Slide-Set-13-Cleaning-Disinfection-Sterilization.pdf

[14] *Documentation Center: Filtering Data.* MathWorks, Natick, MA (2014). Available: http://www.mathworks.com/help/matlab/data_analysis/filtering-data.html

[15] E. Lopo. *libsndfile Library.* Available: http://www.mega-nerd.com/libsndfile/